



JAEA Cesium Workshop: Fukushima Recovery

Molecular Mechanisms and Selectivity of Cs Binding to Clay Minerals

Kevin M. Rosso

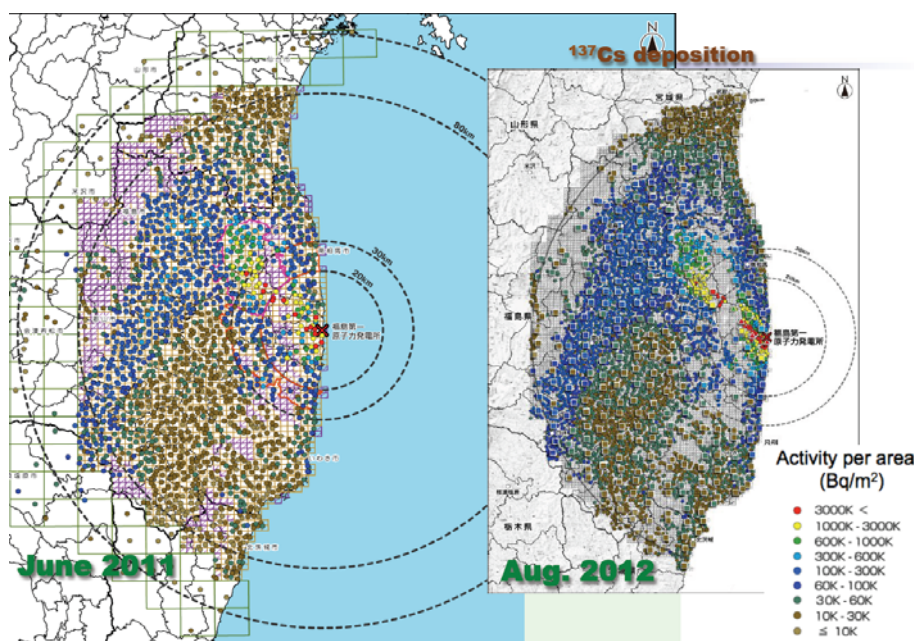
Pacific Northwest National Laboratory, Washington, USA

September 30, 2013



Science Motivation and Need

The ^{137}Cs decontamination effort underway faces challenges remediating vast amounts of farmland soils and forests. R&D is needed for soil cleanup and waste volume reduction. The long-term fate of residual Cs in the environment remains unknown.

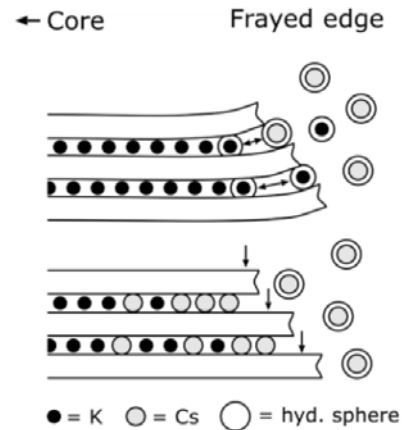
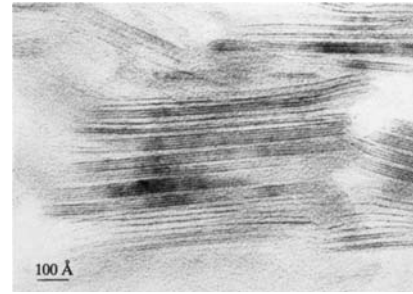


Background

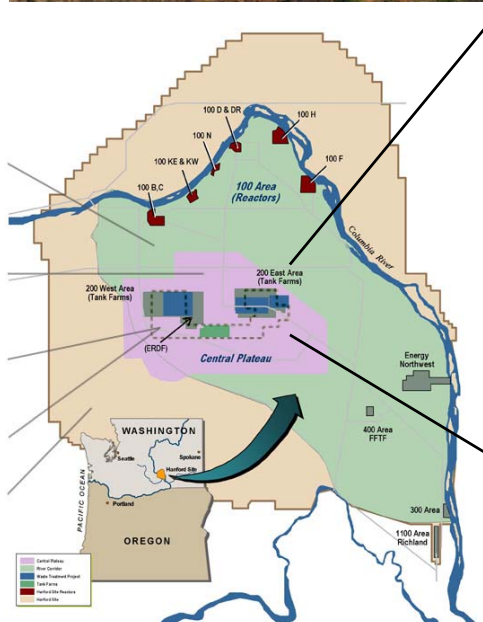
- ▶ **High-affinity Cs⁺ sorption associated with micaceous minerals is well-known**
 - Ion exchange with native interlayer cations at exposed edges and fixation by dehydration and layer collapse

- ▶ **High-affinity site density is low but capacity usually greatly surpasses available Cs⁺**
 - Aqueous transport with depth in soils ultimately limited by conversion from non-specifically to specifically sorbed
 - Long-term mobility depends on particle transport kinetics, or exposure to dissolution or high ionic strength solution

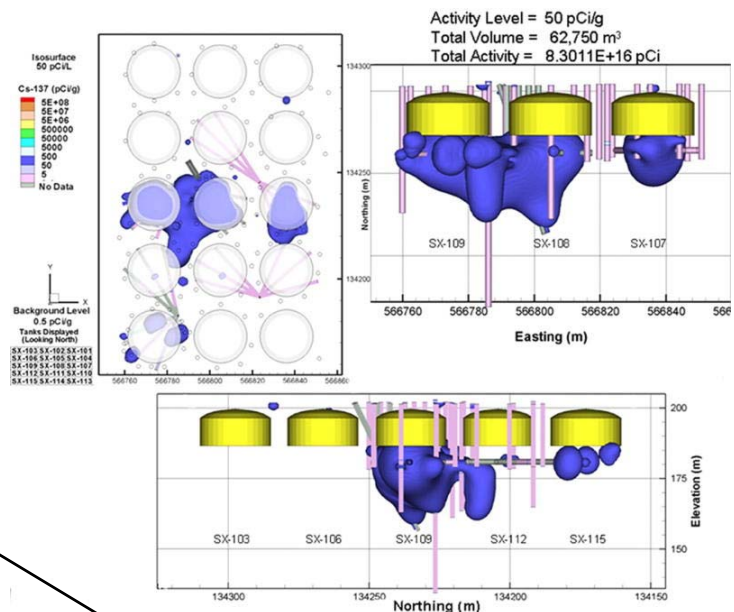
- ▶ **Fixation at high-affinity sites is subject to complex coupled kinetics at multiple scales**
 - Hydrologic transport rates control site access
 - Binding selectivity and strength in micaceous minerals depends on mineralogic characteristics and confined-space diffusive transport kinetics



Hanford Site ¹³⁷Cs Contamination

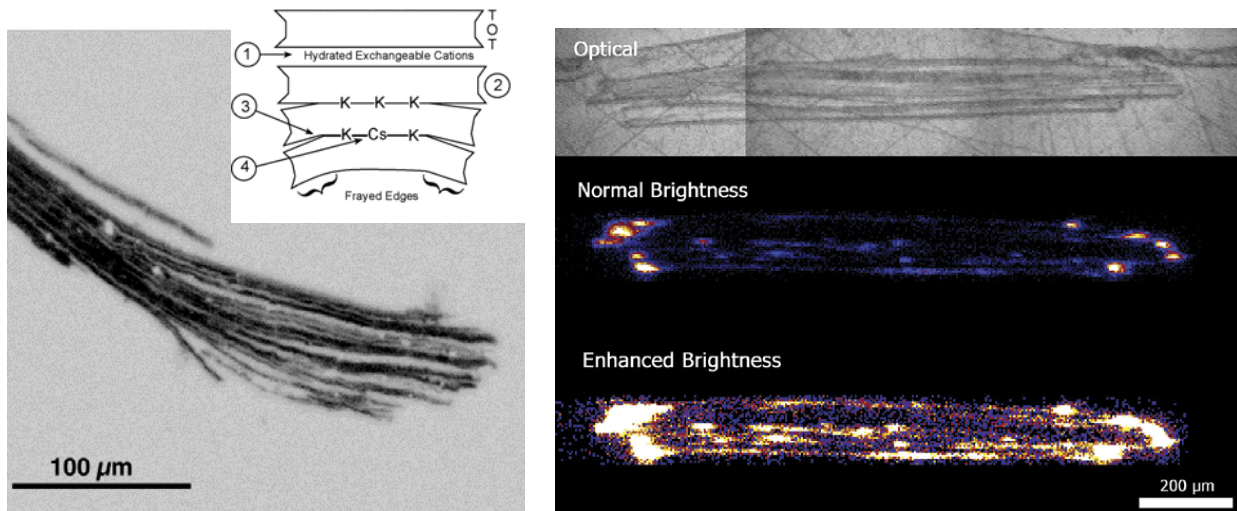


¹³⁷Cs distribution below the SX tank farm



$^{137}\text{Cs}^+$ Selective Sorption to Micaceous Minerals at Hanford

Selective and irreversible Cs^+ exchange into the interlayer of micaceous minerals at Hanford occurs over decadal time-scales as meteoric input slowly transports exchangeable Cs across a thick vadose zone into regions of unsaturated high-affinity sites.



McKinley, Zachara, Heald, Dohnalkova, Newville, Sutton (2004) *Environmental Science and Technology* **38**, 1017-1023.



Science Challenges

Ion exchange/fixation by layered silicates is a dominant subsurface attenuation process for cationic radionuclides and fission products at nuclear accident sites.

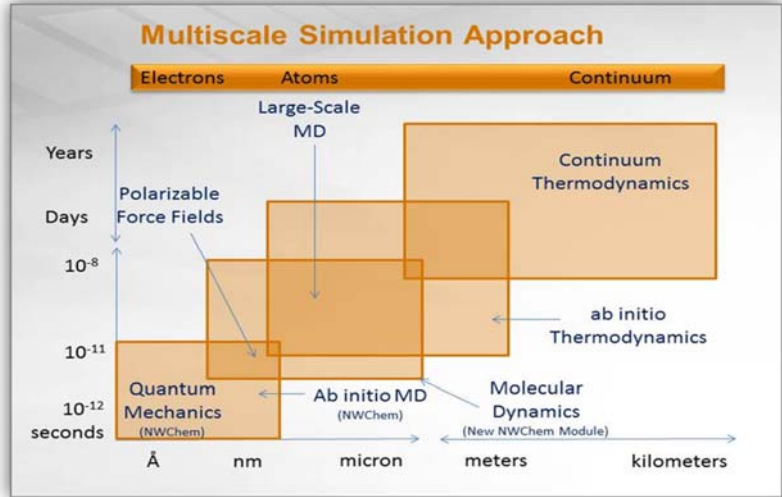
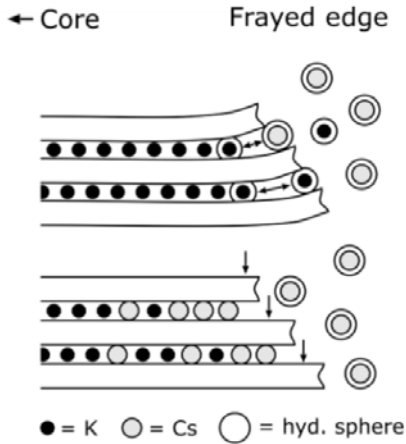
Multicomponent thermodynamic selectivity difficult and tedious to assess experimentally

Theoretical approaches for estimation of selectivity needed for first order projections and experimental interpretation

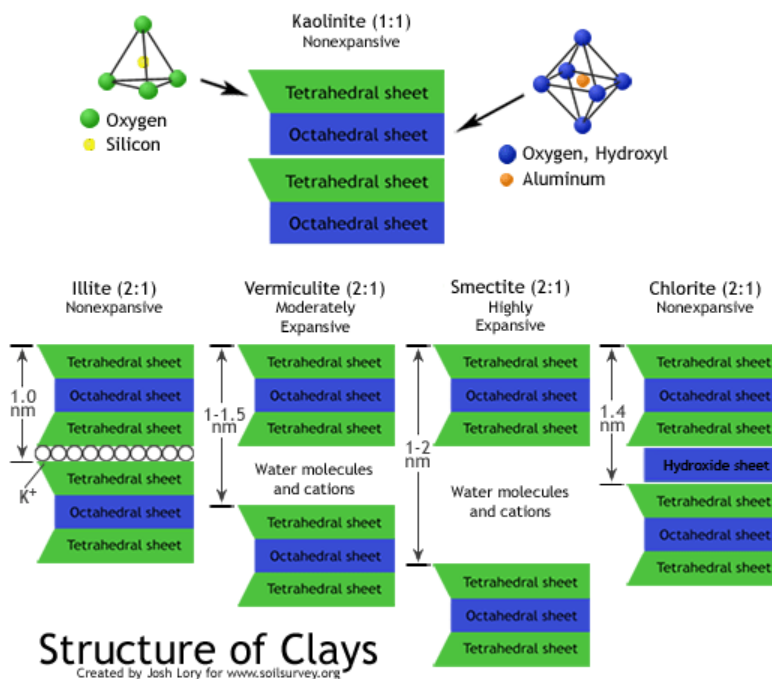


Science Goal

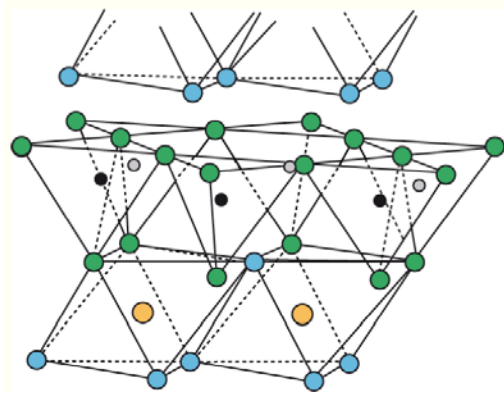
Clean-up and broader impacts lie in developing multi-scale dynamics simulations of Cs uptake by phyllosilicates, from molecular-scale mineralogic exchange processes up to the pore-scale where diffusive transport into and out of high-affinity sites dominates.



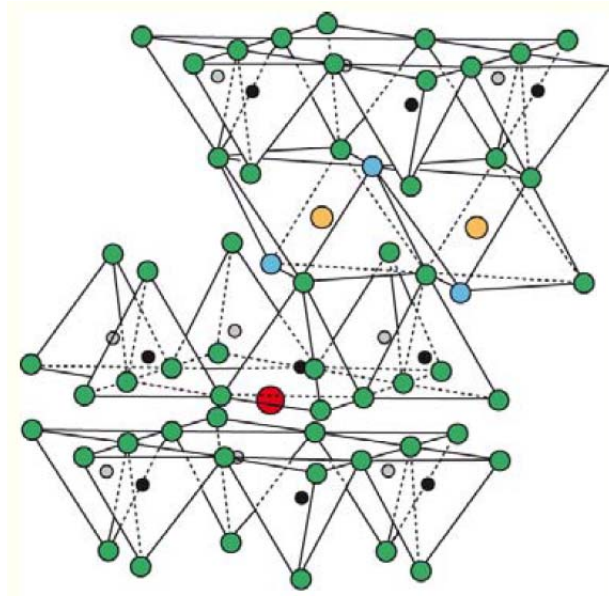
The Basics of Clay Mineral Structures



Site Structure and Layer Charge Depend on Cation Substitutions and Hydroxylation



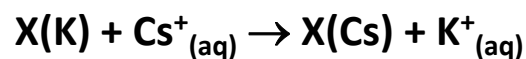
Kaolinite



Illite, Mica

Cation Exchange Energies from DFT

Model the simple exchange reaction



Planewave DFT total energy calculations (zero K)

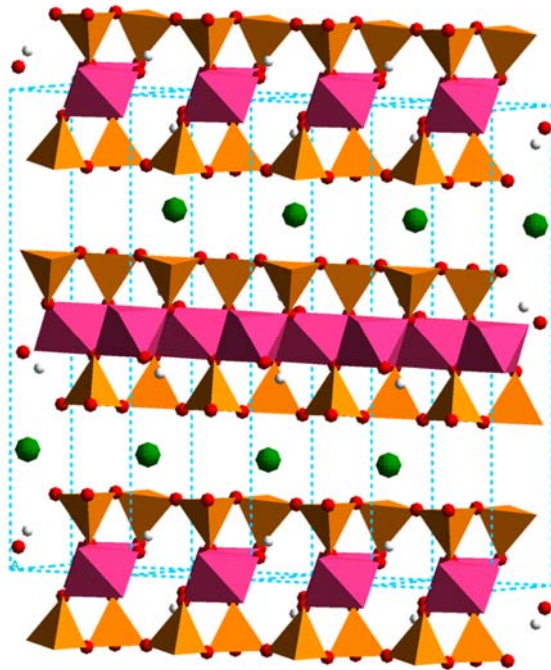
Local site structure, electrostatics, and bonding

Dependence on total layer charge

Dependence on proximity to layer substitution sites

Correct ΔE_{ex} using experimental heats of cation hydration

Muscovite Mica



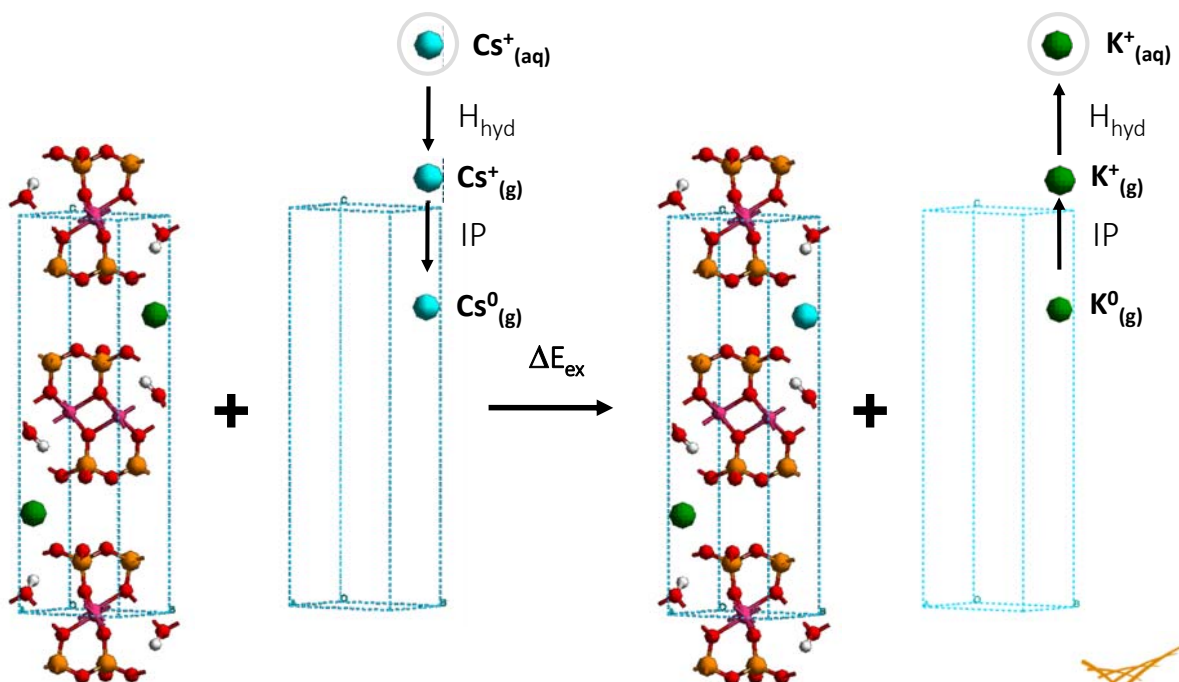
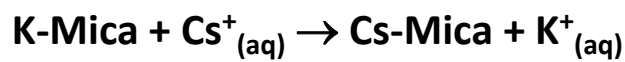
2:1 layer silicate

Dioctahedral mica

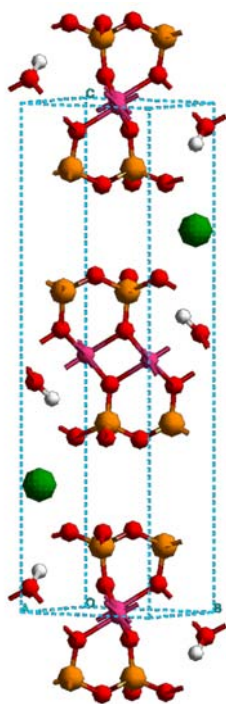
Layer charge (LC) built up
by Al/Si tetrahedral
substitutions



Exchange Energy Computational Strategy



Models to Test LC / Substitution Effects



- $+1$ $+22$ -24
 \downarrow $\underbrace{\hspace{2em}}$ $\underbrace{\hspace{2em}}$
1. $\text{KAl}_2(\text{Si}_4\text{O}_{10})\text{O}_2$
 Slight e^- excess ($\text{LC} = -2$)
 Most tightly bound interlayer cation
 No site distortion
- 2.** $\text{KAl}_2(\text{Si}_4\text{O}_{10})(\text{OH})_2$
 Slight e^- deficit ($\text{LC} = 0$)
 Least tightly bound interlayer cation
 No site distortion
- 3,4.** $\text{KAl}_2(\text{AlSi}_3\text{O}_{10})(\text{OH})_2$
 Formal e^- balance ($\text{LC} = -1$)
 Site distortions

Rosso, Rustad, Bylaska (2001) *Clays and Clay Minerals* 49, 500-513.



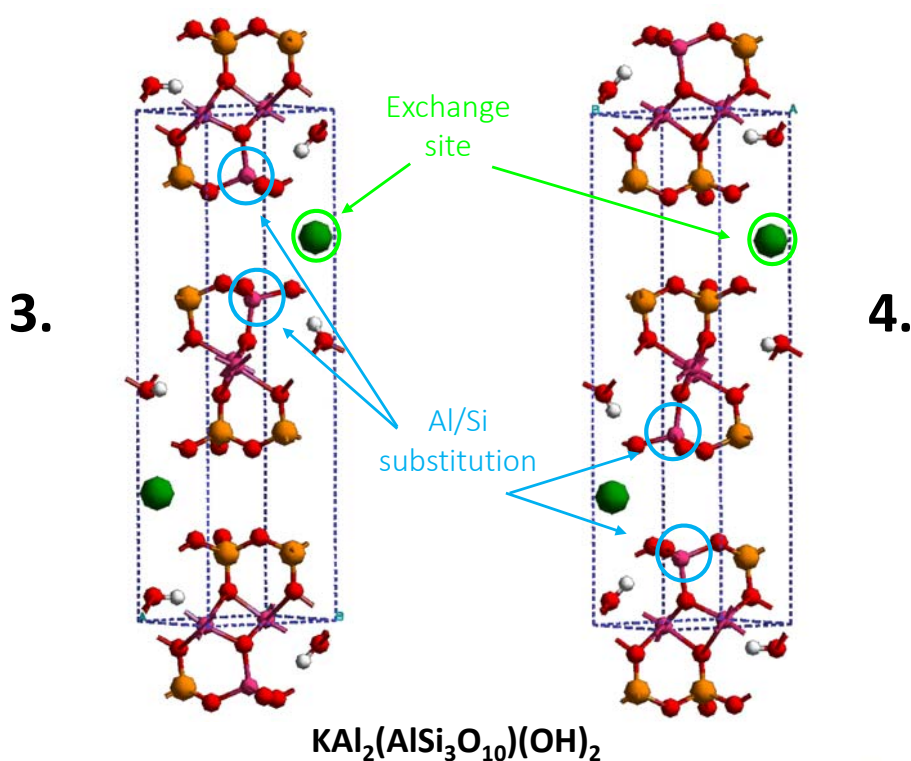
Calculated ΔE_{ex} - No Al/Si Substitution

	1. $\text{KAl}_2(\text{Si}_4\text{O}_{10})\text{O}_2$	2. $\text{KAl}_2(\text{Si}_4\text{O}_{10})(\text{OH})_2$
$\text{X}(\text{K}) + \text{Cs}^0_{(\text{g})} \rightarrow \text{X}(\text{Cs}) + \text{K}^0_{(\text{g})}$	-2.6	13.1
$\text{X}(\text{K}) + \text{Cs}^+_{(\text{aq})} \rightarrow \text{X}(\text{Cs}) + \text{K}^+_{(\text{aq})}$	-5.3	10.4
	$\Delta c = 0.42 \text{ \AA}$	$\Delta c = 0.06 \text{ \AA}$
		(kJ/mol)

Rosso, Rustad, Bylaska (2001) *Clays and Clay Minerals* 49, 500-513.

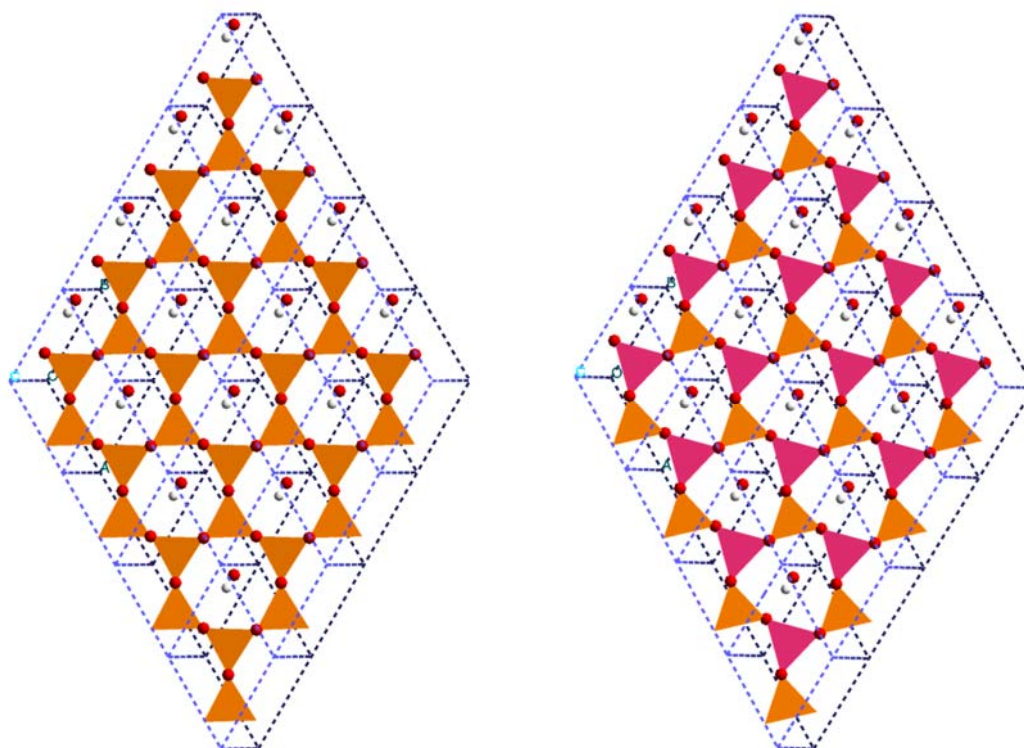


Calculated ΔE_{ex} – Including Al/Si Substitution



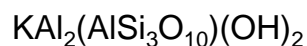
Rosso, Rustad, Bylaska (2001) *Clays and Clay Minerals* 49, 500-513.

Calculated ΔE_{ex} – Including Al/Si Substitution



Rosso, Rustad, Bylaska (2001) *Clays and Clay Minerals* 49, 500-513.

Calculated ΔE_{ex} – Including Al/Si Substitution

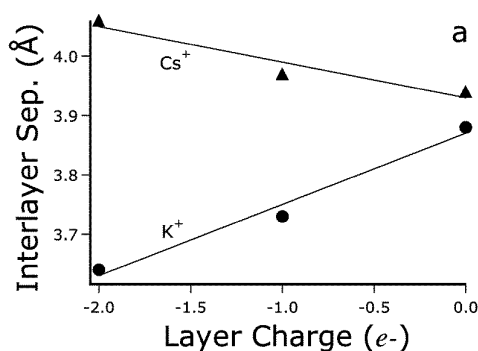


	3. Al/Si at Ex. Site	4. Al/Si at adj. Site
$X(K) + Cs^0_{(g)} \rightarrow X(Cs) + K^0_{(g)}$	18.1	3.0
$X(K) + Cs^+_{(aq)} \rightarrow X(Cs) + K^+_{(aq)}$	15.4	0.3
	$\Delta c = 0.34 \text{ \AA}$	$\Delta c = 0.24 \text{ \AA}$
	(kJ/mol)	

Rosso, Rustad, Bylaska (2001) *Clays and Clay Minerals* 49, 500-513.



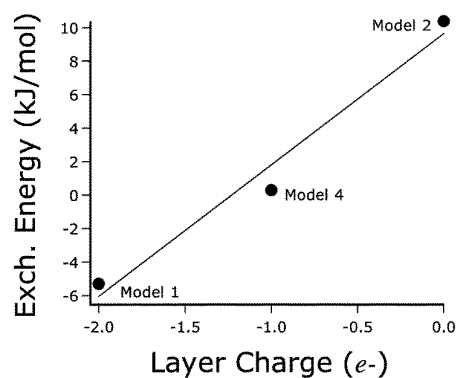
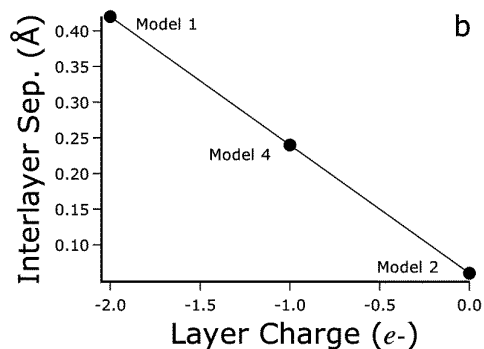
Findings and Implications



Calculated $Cs^+ \rightarrow K^+$ exchange energies derive mostly from cation dehydration energies

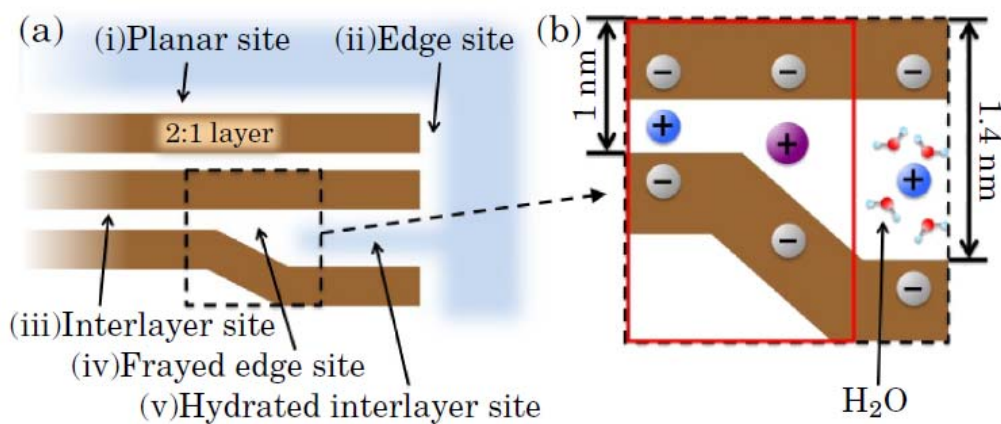
Interlayer site charge distribution appears more important than site "size"

Local changes in the layer charge distribution associated with Al/Si tetrahedral substitutions important



Rosso, Rustad, Bylaska (2001) *Clays and Clay Minerals* 49, 500-513.

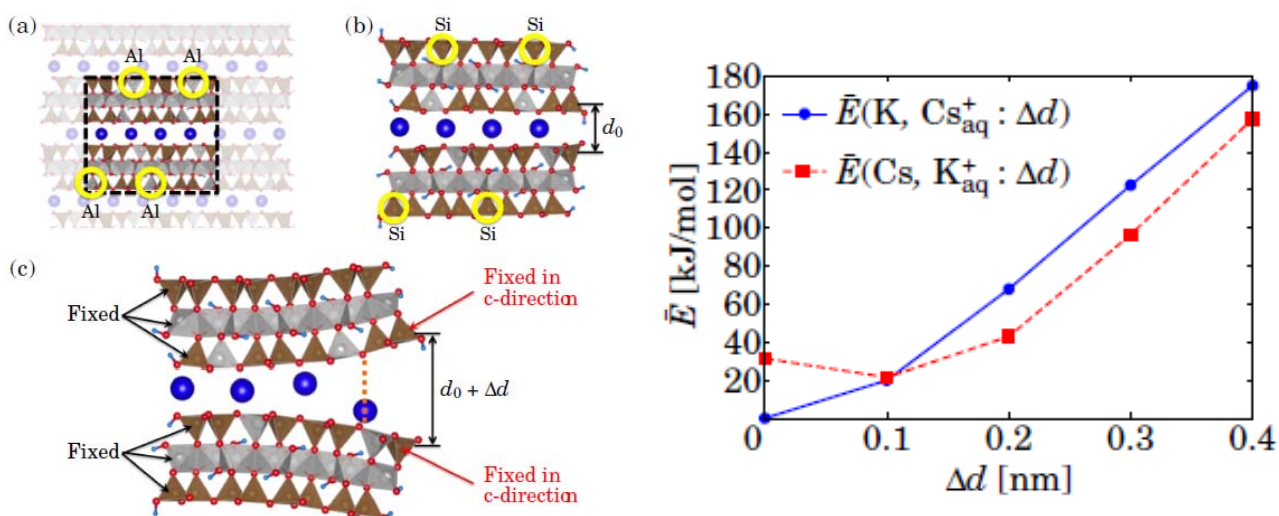
Treatment of Frayed Edge Sites by DFT



Okumura, Nakamura, Machida (2013) *Journal of the Physical Society of Japan* **82**, 033802.



Cs⁺ Selective Binding to Frayed Edge Sites

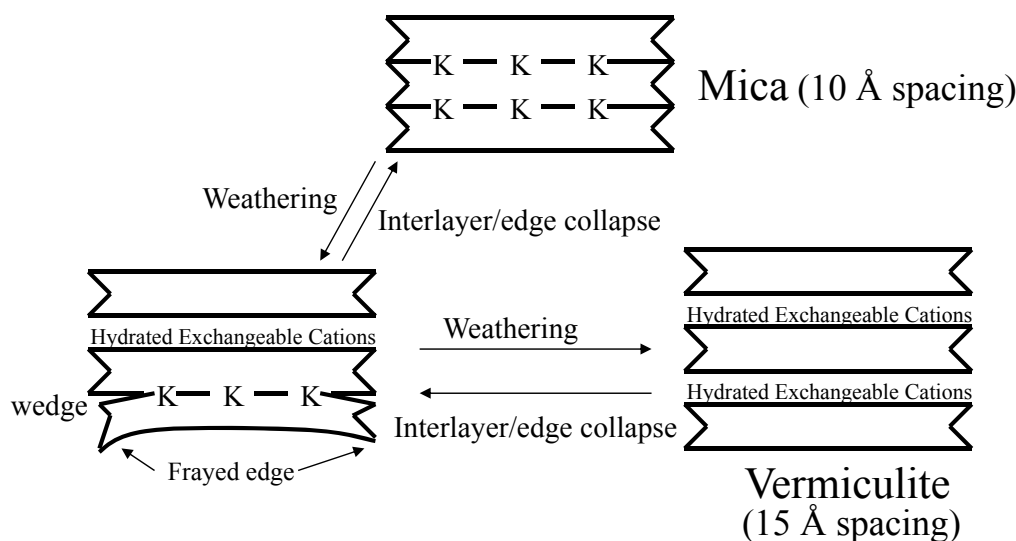


Okumura, Nakamura, Machida (2013) *Journal of the Physical Society of Japan* **82**, 033802.



Continuum-Scale Modeling of Cs⁺ Exchange

2:1 Layer Silicate Weathering and Interlayer/Edge Collapse



Liu, Zachara, Smith, McKinley, Ainsworth (2003) *Geochimica et Cosmochimica Acta* 67, 2893-2912.



Intra-Particle Diffusion Cs⁺ Exchange Model

Interlayer pore phase and surface diffusion:

Edge site

Surface diffusion

Pore phase diffusion

CsX

Cs^+

$Cs^+(aq)$

Cs⁺ diffusion:
$$\frac{\partial q_{Cs}}{\partial t} = \epsilon_p D_p^{Cs} \frac{\partial^2 [Cs^+]_{aq}^{in}}{\partial x^2} + (1 - \epsilon_p) \rho_s D_s^{Cs} \frac{\partial}{\partial x} \left(\varphi(x) \frac{\partial [CsX]^{in}}{\partial x} \right)$$

Cs⁺ exchange:
$$[CsX]^{in} = \frac{K_v^{in} \{Cs^+\}}{\{M^+\} + K_v^{in} \{Cs^+\}}$$

M⁺ diffusion:
$$\frac{\partial q_M}{\partial t} = \epsilon_p D_p^M \frac{\partial^2 [M^+]_{aq}^{in}}{\partial x^2} + (1 - \epsilon_p) \rho_s D_s^M \frac{\partial}{\partial x} \left(\varphi(x) \frac{\partial [MX]^{in}}{\partial x} \right)$$

ϵ_p : intra-particle porosity, ρ_s : solid density, $\varphi(x)$: intra-particle site density

Surface diffusion only:
$$\frac{\partial [Cs]_{ad}^{in}}{\partial t} = (D_s^{Cs} / l^2) \frac{\partial^2 [Cs]_{ad}^{in}}{\partial Y^2}$$

Boundary condition: $[Cs^+]_{ad}^{in} \Big|_{Y=0} = [Cs^+]_{ad}^{ex}(t)$; $\frac{\partial [Cs^+]_{ad}^{in}}{\partial x} \Big|_{Y=1} = 0$; $0 \leq t < +\infty$

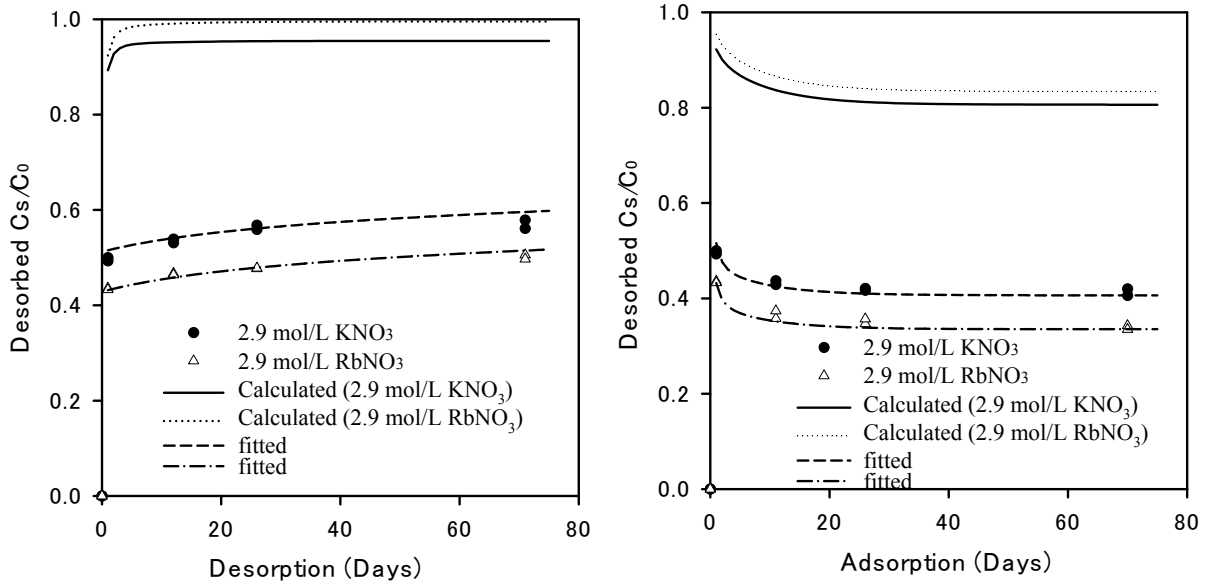
Initial condition: $[Cs^+]_{ad}^{in} \Big|_{t=0} = f(Y)$; $0 \leq Y \leq 1$

Liu, Zachara, Smith, McKinley, Ainsworth (2003) *Geochimica et Cosmochimica Acta* 67, 2893-2912.



Cs⁺ Desorption / Sorption From Hanford Sediment in Rb⁺ and K⁺ Electrolyte

Intra-particle diffusion / Two-site exchange model

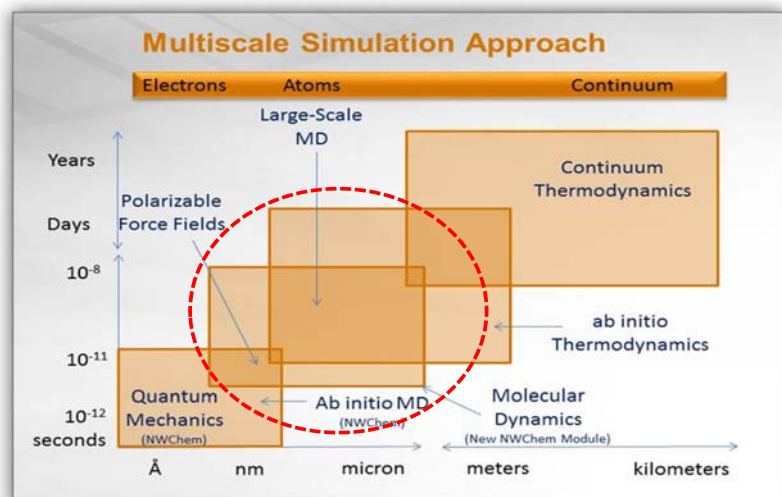
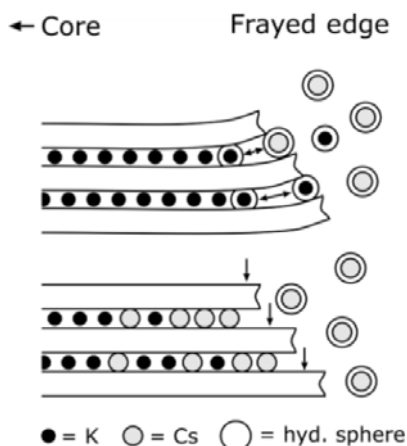


- Fitted: a) $D/l^2 = 1.6 \times 10^{-4} \text{ day}^{-1}$ for both RbNO_3 and KNO_3
 b) 33% of edge site became internal site in KNO_3
 c) 50% of edge site became internal site in RbNO_3

Liu, Zachara, Smith, McKinley, Ainsworth (2003) *Geochimica et Cosmochimica Acta* **67**, 2893-2912.

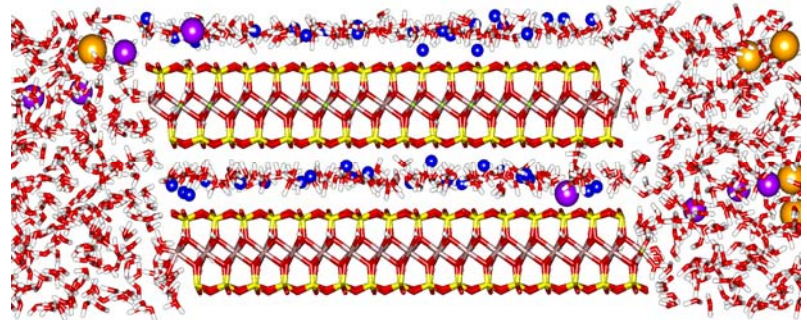
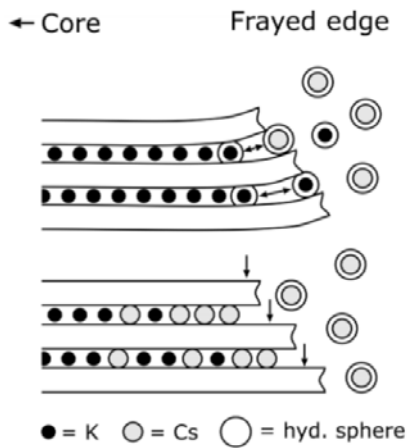
Frontiers to Achieve the Science Goal

Clean-up and broader impacts lie in developing multi-scale dynamics simulations of Cs uptake by phyllosilicates, from molecular-scale mineralogic exchange processes up to the pore-scale where diffusive transport into and out of high-affinity sites dominates.



Frontiers to Achieve the Science Goal

Clean-up and broader impacts lie in developing multi-scale dynamics simulations of Cs uptake by phyllosilicates, from molecular-scale mineralogic exchange processes up to the pore-scale where diffusive transport to high-affinity sites dominates.



- Free energies / equilibrium constants
- Diffusion coefficients
- Sorption / desorption kinetics



Classical Molecular Dynamics Methods

Atoms are represented as point charges which interact via:

$$V(r_{ij}) = \frac{q_i q_j}{r_{ij}} + \phi(r_{ij})$$

→ Coulombic Interactions
→ Short-range Interactions
e.g. electron-cloud repulsion, Van der Waals, bond stretch, etc

Van der Waals Energy

$$E_{VDW}^{ij} = \frac{A}{r_{ij}^{12}} - \frac{B}{r_{ij}^6}$$

Bond Energy

$$E_{bond}^{ij} = k(r_{ij} - r_0)^2$$

Atom trajectories are calculated using Newton's equations of motion:

Verlet Leapfrog scheme

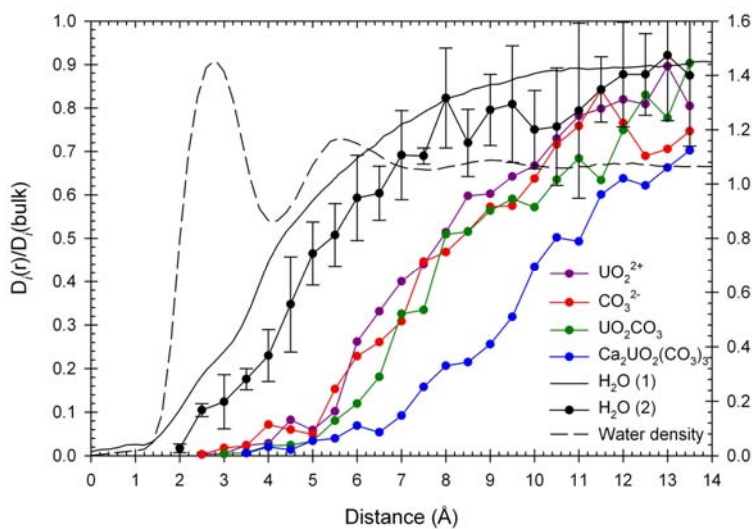
$$v\left(t + \frac{1}{2}\Delta t\right) \leftarrow v\left(t - \frac{1}{2}\Delta t\right) + \Delta t \frac{f(t)}{m}$$

$$r(t + \Delta t) \leftarrow r(t) + v\left(t + \frac{1}{2}\Delta t\right)\Delta t$$

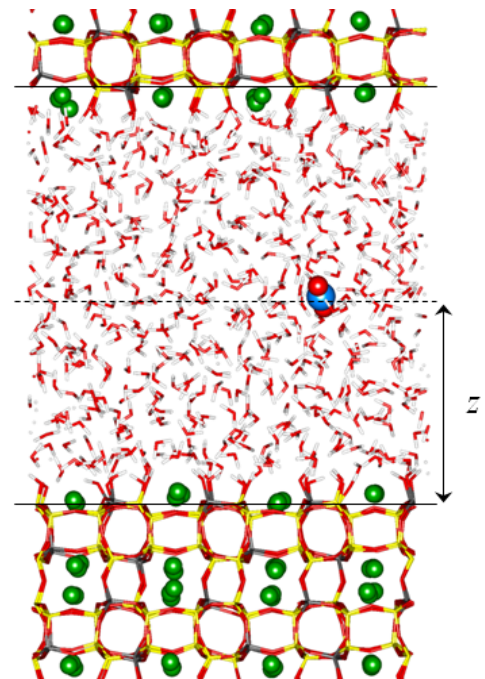


Classical Molecular Dynamics Methods

Constrained molecular dynamics simulations



Rate of decrease in the diffusion coefficients is greater for the larger adsorbing species.



Kerisit S. and Liu C. (2012) *Environ. Sci. Technol.* **46** 1632.



Basic Features of Ab Initio Molecular Dynamics

DFT Equations

$$H\psi_i = \varepsilon_i\psi_i$$

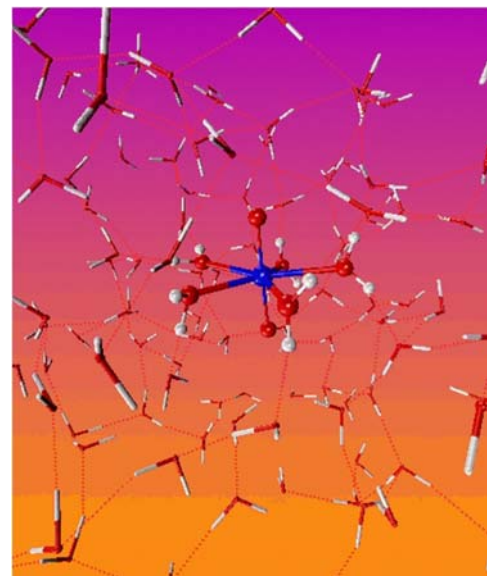
$$H\psi_i(\mathbf{r}) = \left(\begin{array}{l} -\frac{1}{2}\nabla^2 + V_i(\mathbf{r}) + \hat{V}_{NL} + V_H[\rho](\mathbf{r}) \\ +(1-\alpha)V_x[\rho](\mathbf{r}) + V_c[\rho](\mathbf{r}) \end{array} \right) \psi_i(\mathbf{r}) - \alpha \sum_j K_{ij}(\mathbf{r})\psi_j(\mathbf{r})$$

CP dynamics: Ion and wavefunction motion coupled.

Ground state energy $\mu=0$

$$\mu\ddot{\psi}_i = H\psi_i - \sum_{j=1}^{N_e} \lambda_{ij}\psi_j$$

$$M_i\ddot{\mathbf{R}}_i = \mathbf{F}_i \quad \mathbf{F}_i = \sum_{i=1}^{N_e} \langle \psi_i | \frac{\partial H}{\partial \mathbf{R}_i} | \psi_i \rangle$$



Plane-wave basis sets, pseudopotentials are used to solve PDE

Want to do this in ~1 second per step

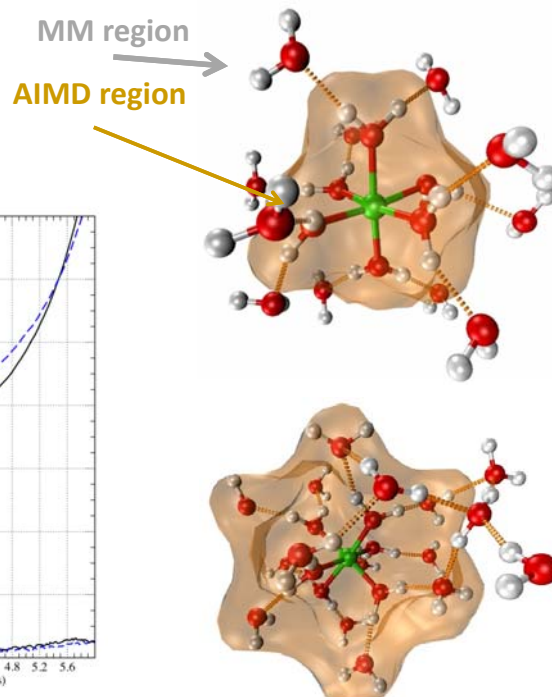
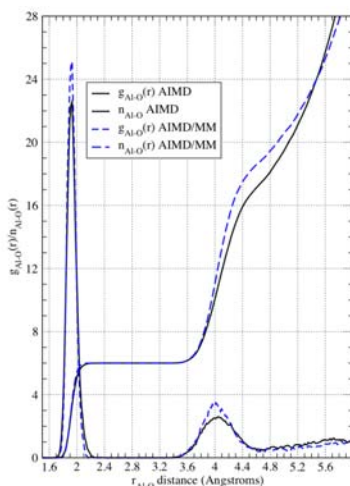
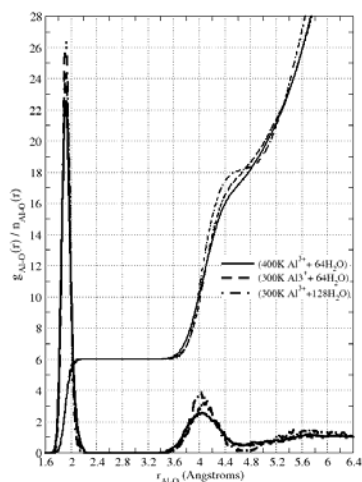


Courtesy of Dr. Eric Bylaska (PNNL)

AIMD / MM – Hydration of Al^{3+}

$$E = E_{\text{AIMD}} + E_{\text{MM}} + E_{\text{AIMD/MM}}$$

Plane-wave basis sets, pseudopotentials are used to solve AIMD equations



1st shell strongly trigonal
Tetrahedral bonding by 2nd hydration shell

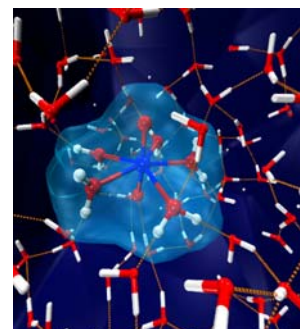
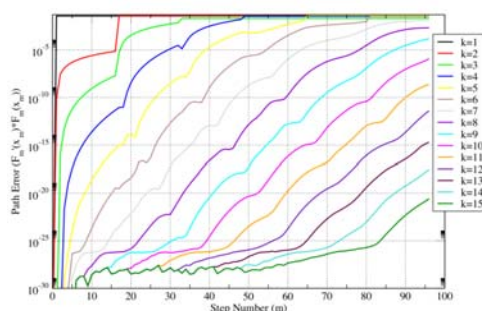
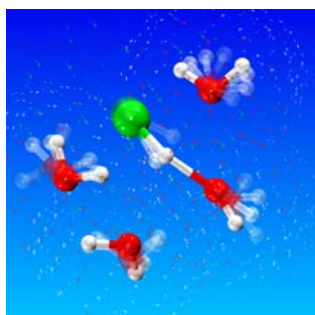


Courtesy of Dr. Eric Bylaska (PNNL)

Rare Event Sampling Methods for AIMD

► Many statistical methods, which are highly parallelizable, characterizing rare events, e.g.

- Metadynamics (Parrinello)
- NEB (Jonsson) and String Methods (E and Vanden-Eijnden)
- Hyperdynamics (Voter)
- Parallel Tempering
- Finite Temperature Transition State Search Methods (e.g. Chandler)
-



Courtesy of Dr. Eric Bylaska (PNNL)

Supercomputing Capabilities at EMSL/PNNL

EMSL's high-performance computational, software, and graphics and visualization capabilities complement the wide range of experimental activities in the environmental molecular sciences. Integration of computing with experiment enables users to greatly accelerate scientific innovation and discovery.

Molecular Science Computing Facility (MSCF)

Capabilities provides to EMSL users with a next-generation 163-teraflop supercomputer Chinook, supported by expert scientific consultants. MSCF also provides state-of-the-art visualization tools and a large data archive



Molecular Science Software Suite (MS³)

MS³ software suite provide users with a comprehensive, integrated set of tools used to understand complex chemical systems at the molecular level.

DOE's premier quantum chemistry software NWChem couples advanced computational chemistry techniques with high-performance, massively parallel computing systems providing the fastest time to solution.

Next Computer Chinook's replacement

EMSL has just [purchased a new 3.4 petaflop \\$17 million supercomputer.](#)

- Theoretical peak processing speed of 3.4 petaflops
- 42 racks 195,840 cores
- 1440 compute nodes with conventional processors and Intel Xeon Phi "MIC" accelerators
- 128 GB memory per node
- FDR Infiniband network
- 2.7 petabyte shared parallel filesystem (60 gigabytes per second read/write)

Pacific Northwest
NATIONAL LABORATORY

Implications and a Path Forward

Science (*widely applicable to other sites*)

- ▶ Improved understanding of Cs⁺ fixation mechanisms and factors controlling its magnitude
 - Structure, charge, electrolyte effects

Applied (*Fukushima directed*)

- ▶ A generalized multi-scale exchange-diffusion model for predictive ion exchange in layered silicates is within reach
 - Mineralogic, structural, and layer charge effects quantified
 - Site occupancy, intra-particle effects, contact time
 - Selective ion effects and chemical potential dependence
- ▶ Equilibrium and rate constants specific to contaminated soil types
- ▶ Capability to forecast future migration and dependence on chemical conditions

Pacific Northwest
NATIONAL LABORATORY